


 Cite this: *Lab Chip*, 2022, 22, 4317

## You will know by its tail: a method for quantification of heterogeneity of bacterial populations using single-cell MIC profiling†

 Natalia Pacocha,<sup>‡a</sup> Marta Zapotoczna,<sup>‡b</sup> Karol Makuch,<sup>‡c</sup> \*<sup>a</sup>  
 Jakub Bogusławski<sup>cde</sup> and Piotr Garstecki \*<sup>a</sup>

Severe non-healing infections are often caused by multiple pathogens or by genetic variants of the same pathogen exhibiting different levels of antibiotic resistance. For example, polymicrobial diabetic foot infections double the risk of amputation compared to monomicrobial infections. Although these infections lead to increased morbidity and mortality, standard antimicrobial susceptibility methods are designed for homogenous samples and are impaired in quantifying heteroresistance. Here, we propose a droplet-based label-free method for quantifying the antibiotic response of the entire population at the single-cell level. We used *Pseudomonas aeruginosa* and *Staphylococcus aureus* samples to confirm that the shape of the profile informs about the coexistence of diverse bacterial subpopulations, their sizes, and antibiotic heteroresistance. These profiles could therefore indicate the outcome of antibiotic treatment in terms of the size of remaining subpopulations. Moreover, we studied phenotypic variants of a *S. aureus* strain to confirm that the profile can be used to identify tolerant subpopulations, such as small colony variants, associated with increased risks for the development of persisting infections. Therefore, the profile is a versatile instrument for quantifying the size of each bacterial subpopulation within a specimen as well as their individual and joined heteroresistance.

 Received 13th March 2022,  
 Accepted 28th September 2022

DOI: 10.1039/d2lc00234e

[rsc.li/loc](https://rsc.li/loc)

### Introduction

Heterogeneity of an infecting bacterial population is an important consideration for the identification of an effective antibiotic treatment.<sup>1,2</sup> Some of the most common infectious diseases are caused by more than one co-colonizing bacterial pathogen, including soft tissue infections, peritonitis, cystic fibrosis, urinary tract infections, and endocarditis.<sup>3</sup> An

estimated 10% of antibiotic-resistant subpopulations is undetectable by current diagnostic tests leading to treatment failure.<sup>4</sup> Moreover, polymicrobial infections doubled the number of amputations in diabetic foot infections,<sup>5</sup> while polymicrobial bloodstream infections were shown to increase the mortality rates from 24 to 47%.<sup>6</sup>

Standard methods for antibiotic susceptibility testing fail to inform on the level of distribution of antibiotic resistance of the entire bacterial population of co-colonizing species. An example of co-infecting pathogens is *Staphylococcus aureus* and *Pseudomonas aeruginosa* abundant and prevailing in the airways and lungs of cystic fibrosis patients.<sup>7,8</sup> Inadequate antibiotic regimens are likely to interfere with the population's complexity in an uncontrollable manner and may promote survival or emergence of resistant subpopulations or remove the non-pathogenic susceptible microflora.<sup>9</sup>

Moreover, in response to environmental stress bacteria can transiently modify their transcriptional profiles or acquire mutations. This type of stress-induced phenotypic heterogeneity has been known since the middle of the 20th century.<sup>10</sup> These mutations often lead to the reduction in metabolic activity or changes to the cell membrane potential that result in an altered phenotypes, such as a longer lag time, increased tolerance to antibiotics. Stress-

<sup>a</sup> Institute of Physical Chemistry, Polish Academy of Sciences, Kasprzaka 44/52, 01-224 Warsaw, Poland. E-mail: [kmakuch@ichf.edu.pl](mailto:kmakuch@ichf.edu.pl), [pgarstecki@ichf.edu.pl](mailto:pgarstecki@ichf.edu.pl)

<sup>b</sup> Department of Molecular Microbiology, Institute of Microbiology, Faculty of Biology, Biological and Chemical Research Centre, University of Warsaw, Żwirki i Wigury 101, 02-089 Warsaw, Poland

<sup>c</sup> International Centre for Translational Eye Research, Institute of Physical Chemistry, Polish Academy of Sciences, Kasprzaka 44/52, 01-224 Warsaw, Poland

<sup>d</sup> Department of Physical Chemistry of Biological Systems, Institute of Physical Chemistry, Polish Academy of Sciences, Kasprzaka 44/52, 01-224 Warsaw, Poland

<sup>e</sup> Laser & Fiber Electronics Group, Faculty of Electronics, Wrocław University of Science and Technology, Wybrzeże Wyspińskiego 27, 50-370 Wrocław, Poland

† Electronic supplementary information (ESI) available: Scheme of optical setup, exemplary autofluorescence signals, growth curves of normal colony and small colony variant phenotype, precision of scMIC curve determination, list of bacteria strains tested towards native fluorescence intensity, breakpoint concentrations of NCPs and SCVs, details regarding determination of scMIC profile. See DOI: <https://doi.org/10.1039/d2lc00234e>

‡ These authors contributed equally.







**Fig. 1** Experimental determination of scMIC profiles of polymicrobial samples of pre-mixed *S. aureus* MSSA47 and *P. aeruginosa* PAO1; a) schematic overview of the workflow for label-free determination of scMIC profile, b) MIC values determined by standard microdilution method for ciprofloxacin and tobramycin against studied strains, c and d) scMIC profiles of pre-mixed samples determined as a fraction of positive droplets, a function of antibiotic concentration measured based on scattered light (grey line) and autofluorescence (green line) intensity. The breakpoints values for both pre-mixed samples are 1.5 and 4  $\mu\text{g mL}^{-1}$  for ciprofloxacin and tobramycin, respectively. Statistical treatment of error analysis is described in detail in ESI.†

more details). We define scMIC by the concentration that inhibits all bacteria (here determined at the point where  $f_+ \leq 0.1\%$ ). The scMIC for the samples made of a pre-mixed population was determined at 1.5  $\mu\text{g mL}^{-1}$  for ciprofloxacin and 4  $\mu\text{g mL}^{-1}$  for tobramycin [Fig. 1c and d], which corresponded to the breakpoint concentrations of the less susceptible strain, as verified by comparing to the breakpoints values determined for single strains using the standard microdilution method [Fig. 1b]. It is worth mentioning that Artemova *et al.*<sup>24</sup> determined scMIC in a similar way, although by plating cells on agar and counting colony growth. This could lead to different scMIC values due to the limited amount of antibiotic in droplets.<sup>26</sup> The application of an autofluorescence detector allowed for discrimination between bacterial subpopulations and for quantitative estimation of the proportion of either strain across antibiotic concentrations in a studied sample. Droplets containing *S. aureus* were detected by scattering whilst *P. aeruginosa* containing could be detected by both detectors. At the region of low antibiotic concentrations (up to 0.125  $\mu\text{g mL}^{-1}$  for ciprofloxacin, or 0.5  $\mu\text{g mL}^{-1}$  for tobramycin) the  $f_+$  values from scattered light corresponded to the growth of the entire mixed bacterial population [Fig. 1c and d]. The scMIC profiles determined by scattering and autofluorescence for ciprofloxacin were superimposed above the *S. aureus* breakpoint  $c$  of ca. 0.5  $\mu\text{g mL}^{-1}$ , thus represented subpopulation of recoverable *P. aeruginosa* [Fig. 1c]. The scMIC profile for tobramycin

above the 1  $\mu\text{g mL}^{-1}$  was determined only from scattering as no autofluorescence could be detected above this concentration, suggesting the remaining recoverable cells were all *S. aureus*. We estimated the proportions of both species in the samples based on the fraction of positive droplets where bacteria were not treated with antibiotic. To obtain the sizes of *P. aeruginosa* populations we designated the ratios of the droplets recognized by high native fluorescence intensity to the positive droplets detected by the high signal of scattered light. We determined *P. aeruginosa* population at 50%  $\pm$  5% and 9%  $\pm$  1% for samples treated with ciprofloxacin and tobramycin, respectively. The remaining portions of the samples correspond to the sizes of *S. aureus* population.

These results demonstrate the effectiveness of our method in the determination of the scMIC profile of a sample consisting of two bacterial subpopulations. Moreover, we observed that scMIC profiles obtained using scattering alone are sufficient to inform on the population complexity (existence of more than one subpopulation of bacteria with different level of antibiotic tolerance). Yet, in mixed populations of a large disproportion in subpopulation sizes (one strain over the other), autofluorescence is essential to discriminate.

#### scMIC profiles of normal cells and small colony variants

Next, we used scattering-based detection to determine the scMIC profiles of phenotypically heterogeneous samples of a



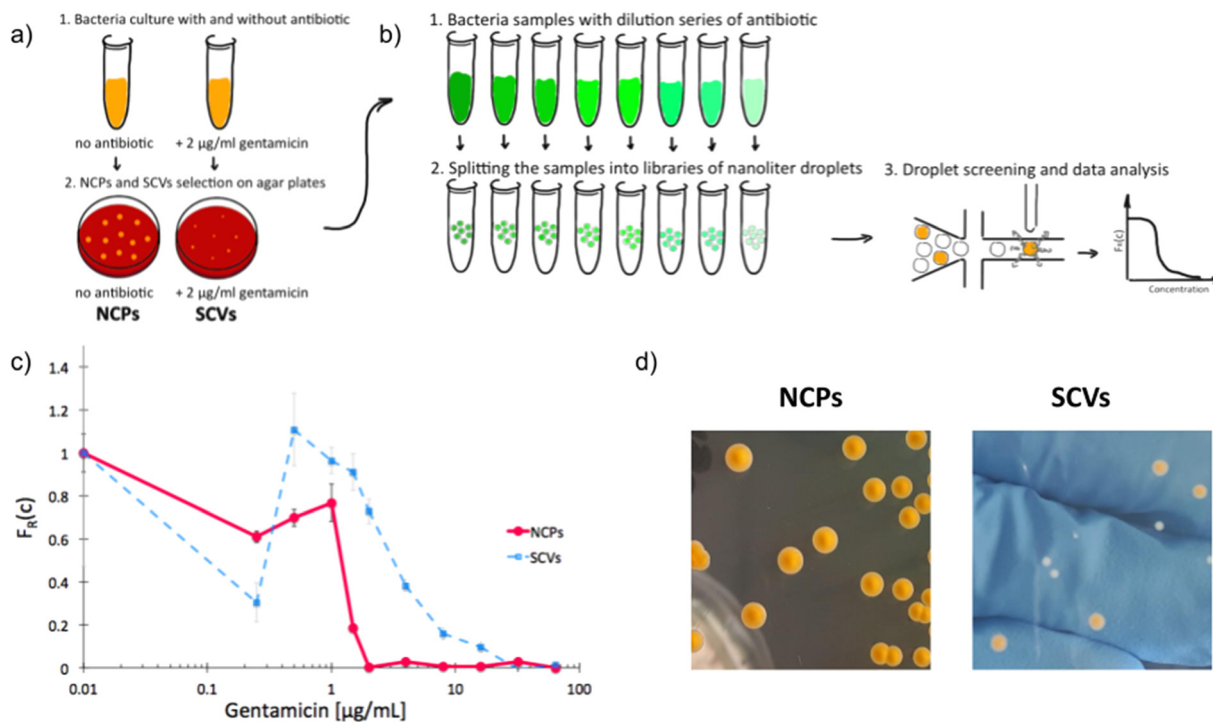


**Fig. 2** Experimental determination of single-cell MIC profile for *Staphylococcus aureus* of normal colony phenotype (NCPs) and small colony variants (SCVs); a) schematic overview of the experimental workflow of SCVs triggering and b) determination of scMIC including sample analysis towards phenotypic heterogeneity, c) comparison of single-cell MIC profiles determined for NCPs (red) and SCVs (blue), d) photographs of representative NCP and SCV colonies on tryptic soy agar, respectively. Statistical treatment of error analysis is described in detail in ESI.†

clonal strain. We selected normal morphology colonies (normal colony phenotype, NCP) of strain *S. aureus* SH1000 grown under optimal conditions, as well as colonies representing the small colony variant (SCV) phenotype, which we triggered with gentamicin [Fig. 2a]. Isolated SCV colonies were characterized by phenotypic changes, including aminoglycoside tolerance, small colony size, longer lag time, and reduced pigmentation [Fig. 2d, S3†]. Both populations, consisting of cells harvested from either NCP or SCV colonies, were separately subjected to scMIC testing [Fig. 2b] and the respective scMIC profiles were determined (see Materials and methods for more details). The NCP population required 2  $\mu\text{g mL}^{-1}$  for the inhibition of the entire population while the scMIC of the SCV population was determined at 32  $\mu\text{g mL}^{-1}$  [Fig. 2c]. Both scMIC values determined for either NCP or SCV were consistent with the breakpoint concentrations measured for the respective populations using the standard microdilution method [Table S2†].

Distinctive scMIC profiles, consisting of two regions, were observed for NCPs and SCVs [Fig. 2c]. The region of low antibiotic concentrations (up to gentamicin of *ca.* 1  $\mu\text{g mL}^{-1}$ ) with a slowly decaying fraction of recovering bacteria  $F_R(c)$  was similar for both, NCP and SCV. The second region which we referred to as a transition region started at gentamicin of 1  $\mu\text{g mL}^{-1}$  and was different in both populations. For NCPs the transition region ended at 2  $\mu\text{g mL}^{-1}$  and had a sharp decline, while for SCVs it reached 32  $\mu\text{g mL}^{-1}$  and had a

much milder slope. Therefore, the transition region for SCVs was about 16 times broader than for NCPs. In this sense our SCVs population was 16 times more resistant than NCPs, suggesting it consists of bacterial cells of larger distribution of antibiotic susceptibility. In the low antibiotic region with a high proportion of positive droplets the  $F_R(c)$  values fluctuations were observed. They could be related to the decreased stability of non-empty droplets (droplets containing bacteria) likely to be caused by the cell aggregation, which is characteristic of the strain *S. aureus* SH1000.

#### 'Tails' in the scMIC profiles

As we characterized the scMIC profiles of either NCPs or gentamicin-triggered SCVs, we wanted to investigate if they could determine their respective contribution within pre-mixed populations of a known proportion. The homogenous suspensions of NCPs and SCVs were combined into heterogeneous mixtures consisting of either 12% SCVs or 50% of SCVs and the remaining portion of NCPs, respectively [Fig. 3a]. As expected, the scMIC profiles of mixtures were combinations of profiles of either population. The profile of 12% SCV declined sharply in the transition region around 1  $\mu\text{g mL}^{-1}$  to the  $F_R(c)$  value of 0.08 and continued on with a minimal reduction in the shape of a tail between 1 and 8  $\mu\text{g mL}^{-1}$ . The height of the tail at 0.08 directly corresponded to the size of SCV subpopulation and it amounts to 8% [Fig. 3b].





**Fig. 3** Single-cell MIC measurement of mixtures of phenotypic variants of *S. aureus* SH1000; a) schematic workflow of sample preparation, b) single-cell MIC profile of phenotypically heterogeneous mixtures containing respectively 12% (solid pink) and 50% (dotted purple) small colony variants (SCV) mixed with normal phenotype cells (NCPs). Statistical treatment of error analysis is described in detail in ESI.†

Whereas the scMIC distribution for the mixture of 50% SCV was broader, yet equally sharp starting at  $2 \mu\text{g mL}^{-1}$  down to  $F_R(c)$  ca. 0.37 and continuing as a tail ending at  $16 \mu\text{g mL}^{-1}$  [Fig. 3b]. Based on the height of the tail we estimated the SCV cells at 37% of the entire population. The difference between 50% and 37% follows from the

precision of our method that we discuss in “Method precision” below.

These results indicate that the tail represents the size of SCVs subpopulation, whether it is low height corresponding to the low SCV content or high with a larger size subpopulation of tolerant bacteria. Consequently, the shape



**Fig. 4** Single-cell MIC profiles of *S. aureus* dispersed from the biofilm. a) Schematic workflow of biofilms formation together with NCPs and SCVs selection in the absence (top) and presence (bottom) of gentamicin; b) heterogeneity profiles for NCPs (solid red) and SCVs (dotted blue) isolated from a biofilm cultured for 24 hours in the presence of gentamicin; c) scMIC profiles of biofilms cultured in the presence (dotted purple) and absence (solid pink) of gentamicin; d) the tails of scMIC profiles shown in c). Statistical treatment of error analysis is described in detail in ESI.†











- 16 H. Nicoloff, K. Hjort, B. R. Levin and D. I. Andersson, The high prevalence of antibiotic heteroresistance in pathogenic bacteria is mainly caused by gene amplification, *Nat. Microbiol.*, 2019, **4**, 1–13.
- 17 H. Nicoloff, K. Hjort, B. R. Levin and D. I. Andersson, The high prevalence of antibiotic heteroresistance in pathogenic bacteria is mainly caused by gene amplification, *Nat. Microbiol.*, 2019, **4**, 504–514.
- 18 D. Belikova, A. Jochim, J. Power, M. T. G. Holden and S. Heilbronner, “Gene accordions” cause genotypic and phenotypic heterogeneity in clonal populations of *Staphylococcus aureus*, *Nat. Commun.*, 2020, **11**(11), 1–15.
- 19 J. Q. Boedicker, L. Li, T. R. Kline and R. F. Ismagilov, Detecting bacteria and determining their susceptibility to antibiotics by stochastic confinement in nanoliter droplets using plug-based microfluidics, *Lab Chip*, 2008, **8**, 1265–1272.
- 20 L. Baraban, *et al.* Millifluidic droplet analyser for microbiology, *Lab Chip*, 2011, **11**, 4057–4062.
- 21 X. Liu, *et al.* High-throughput screening of antibiotic-resistant bacteria in picodroplets, *Lab Chip*, 2016, **16**, 1636–1643.
- 22 T. S. Kaminski, O. Scheler and P. Garstecki, Droplet microfluidics for microbiology: Techniques, applications and challenges, *Lab Chip*, 2016, **16**, 2168–2187.
- 23 A. M. Kaushik, *et al.* Accelerating bacterial growth detection and antimicrobial susceptibility assessment in integrated picoliter droplet platform, *Biosens. Bioelectron.*, 2017, **97**, 260–266.
- 24 T. Artemova, Y. Gerardin, C. Dudley, N. M. Vega and J. Gore, Isolated cell behavior drives the evolution of antibiotic resistance, *Mol. Syst. Biol.*, 2015, **11**, 822.
- 25 F. Lyu, *et al.* Phenotyping antibiotic resistance with single-cell resolution for the detection of heteroresistance, *Sens. Actuators, B*, 2018, **270**, 396–404.
- 26 O. Scheler, *et al.* Droplet-based digital antibiotic susceptibility screen reveals single-cell clonal heteroresistance in an isogenic bacterial population, *Sci. Rep.*, 2020, **10**, 3282.
- 27 N. Pacocha, *et al.* High-Throughput Monitoring of Bacterial Cell Density in Nanoliter Droplets: Label-Free Detection of Unmodified Gram-Positive and Gram-Negative Bacteria, *Anal. Chem.*, 2020, **93**, 843–850.
- 28 Y. C. Wu, *et al.* Autofluorescence imaging device for real-time detection and tracking of pathogenic bacteria in a mouse skin wound model: preclinical feasibility studies, *J. Biomed. Opt.*, 2014, **19**, 085002.
- 29 W. K. Philipp-Dormston and M. Doss, Comparison of Porphyrin and Heme Biosynthesis in Various Heterotrophic Bacteria, *Enzyme*, 1973, **16**, 57–64.
- 30 C. D. Cox and P. Adams, Siderophore activity of pyoverdinin for *Pseudomonas aeruginosa*, *Infect. Immun.*, 1985, **48**, 130–138.
- 31 A. M. Edwards, Phenotype switching is a natural consequence of *Staphylococcus aureus* replication, *J. Bacteriol.*, 2012, **194**, 5404–5412.
- 32 P. M. Molyneux, S. Kilvington, M. J. Wakefield, J. I. Prydal and N. P. Bannister, Autofluorescence Signatures of Seven Pathogens: Preliminary in Vitro Investigations of a Potential Diagnostic for *Acanthamoeba Keratitis*, *Cornea*, 2015, **34**, 1588–1592.
- 33 H. K. Peguda, *et al.* The Autofluorescence Patterns of *Acanthamoeba castellanii*, *Pseudomonas aeruginosa* and *Staphylococcus aureus*: Effects of Antibiotics and Tetracaine, *J. Pathog.*, 2021, **10**, 894.

